Loudspeaker Array-Based Auralization of Electric Vehicle Noise in Living Environments

FORUM ACUSTICUM EURONOISE 2025

LOUDSPEAKER ARRAY-BASED AURALIZATION OF ELECTRIC VEHICLE NOISE IN LIVING ENVIRONMENTS

Leon Müller* **Jens Ahrens** **Wolfgang Kropp**

Division of Applied Acoustics, Chalmers University of Technology, Sweden

ABSTRACT

With the ongoing shift towards electromobility, electric vehicle warning sounds are becoming increasingly prevalent in urban areas, and listening experiments investigating the possible influence of such sounds on human health and well-being are needed. For this purpose, we recently presented an electric vehicle auralization toolbox, which we extend with this paper by implementing a speaker-based reproduction approach in our *Living Room Lab*. This lab consists of two adjacent rooms coupled with a window: one designed to resemble a typical living space and one equipped with an array of 24 loudspeakers. Employing sound field synthesis, we use these loudspeakers to recreate the sound field of an outdoor electric vehicle pass-by in the sending room, which then propagates through the window and results in a spatially accurate sound field in the receiving living room. In this study, we assess different array setups and synthesis strategies to mitigate time structure distortions of vehicle passages caused by the finite aperture of the loudspeaker array. Modeling the sound propagation between the two coupled rooms, we numerically compare these methods to a simulated continuous outdoor pass-by and perceptually evaluate the results by auralizing the simulated sound fields at a listening position.

Keywords: *Electric Vehicles, Auralization, Wave Field Synthesis, Indoor Noise*

**Corresponding author*: *leon.mueller@chalmers.se.*

1. INTRODUCTION

With the current transition to electromobility, electric vehicles (EVs) are becoming increasingly popular, especially in urban environments. Since EVs typically emit little sound at low driving speeds [1], regulations require manufacturers to implement acoustic vehicle alerting systems (AVAS), i.e., a loudspeaker that radiates artificial sounds indicating the vehicle's driving behaviors to pedestrians and other vulnerable road users [2]. While these AVAS sounds have been investigated in terms of detectability and localization efficiency [3, 4], there is only a limited number of studies on their environmental noise impact [5, 6].

Even though the current EU regulations allow AVAS levels of up to 75 dBA at 2 m distance [2], measurements presented in [7] indicate that the AVAS levels of the evaluated electric vehicles tend to rather be situated at the lower regulation limit of 50 dBA for 10 km/h and 56 dBA for 20 km/h at 2 m distance. Due to the limited radiation capabilities of typically used AVAS loudspeakers and the requirements set by the regulations, current AVAS sounds tend to have less low-frequency content than combustion noise, which means that electric vehicle warning sounds might be less audible indoors behind a modern window and facade, than combustion engine noise. However, humans on balconies, in gardens, or in living spaces with open windows could still be exposed to the sound of EVs slowly passing on a nearby road, especially in slow-driving areas such as residential neighborhoods. Evaluating the human response to these sounds can help identify AVAS signals that potentially have less negative impact on health and well-being. While such human subject experiments could be performed in situ, i.e., exposing humans to sounds from actual electric vehicles driving by a building, conducting such a study would be a high effort with limited con-

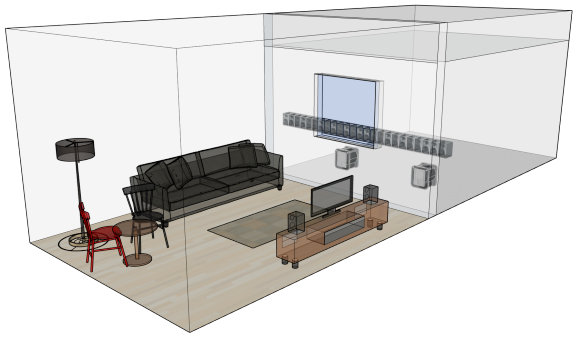

Figure 1: Model of the Chalmers *Living Room Lab* with a linear array of 24 loudspeakers in the sending room.

trol over the environment. Instead, such experiments can be conducted in a laboratory environment using methods of virtual acoustics, allowing the simulation of arbitrary vehicle passages while having complete control over the acoustic environment.

One challenge of conducting human subject experiments in virtual acoustic environments is the need for a sophisticated and validated auralization method to produce reliable experiment results that are applicable to real-life scenarios. For this purpose, we recently introduced an electric vehicle auralization toolbox [7] that we used to evaluate the localization accuracy of different electric vehicle sounds in a static parking lot scenario [4] as well as the influence of AVAS directivity on pass-by speed perception [8]. This paper extends this auralization method by implementing and validating a speaker-based reproduction approach in our Living Room Lab. The following sections introduce this laboratory setup (Sec. 2.1) and present a speaker-based sound field synthesis approach (Sec. 2.2), a numerical model to predict (Sec. 2.4) and auralize (Sec. 2.5) the outcome of different loudspeaker array geometries, as well as a perceptual evaluation of the reproduction method (Sec. 2.6).

2. METHODS

2.1 Laboratory Setup

Figure 1 shows a visualization of the Chalmers *Living Room Lab*, consisting of two acoustically isolated rooms. Both rooms are separated by a gypsum double wall with a 1.2 m x 1 m aluminum double glass window. One of the rooms, the sending room, is equipped with a loudspeaker array right in front of the separating window. The receiving room is furnished to match the look and feel of a typical living room. The fundamental concept behind this laboratory setup is that the loudspeaker array in the sending room projects the incoming sound field of an outdoor sound source to the surface of the separating window. The sound then propagates through the window, resulting in a spatially accurate sound field in the receiving room. Including a physical wall and window in the reproduction has the advantage that these aspects of the propagation and the incidence angle-dependent sound transmission do not need to be simulated, and, no matter how accurate the reproduction in the sending room is, the propagation through and radiation by the window will be authentic.

2.2 Wave Field Synthesis

To project the incoming sound field of an outdoor point source to the window in the sending room, wave field synthesis (WFS) is used [9, 10] and driving functions for each loudspeaker position are derived by calculating the pressure gradient in the normal direction of each speaker membrane and applying the corresponding distance attenuation and runtime delay. Spectral artifacts caused by the fact that the loudspeaker arrays are one-dimensional rather than two-dimensional are compensated by including a prefilter, according to [11].

Source movement is implemented through the concept of moving greens functions, i.e., by discretizing the source trajectory depending on the desired source velocity, v, and the simulation sample rate, f_s, in steps of v/f_s m. Each of these discrete source positions is then used to calculate a separate set of WFS loudspeaker driving functions for each audio sample of the source signal, which is then applied through sample-wise time-variant filtering. This results in physically accurate modeling of the source movement, including the Doppler shift. Even though a monopole source is assumed in the derivation of the WFS, approximate sound source directivities can be implemented by including the spectral magnitude of the desired directivity for the relative angle between each loudspeaker and each discrete source position in the individual driving functions. Additionally, the outdoor sound propagation modeling is refined by including distance- and frequency-dependent air absorption [12] and von Kármán atmospheric turbulences [13] through time-variant filtering of the source signal.

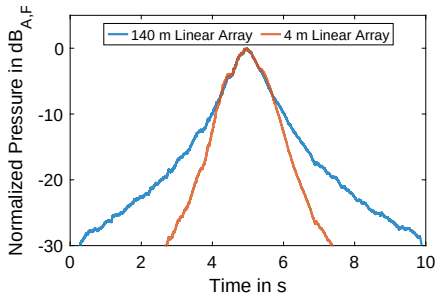

Figure 2: Normalized sound pressure level obtained from free-field simulation of 50 km/h vehicle passage at 7.5 m distance, synthesized via a linear loudspeaker array of 4 m and 140 m length.

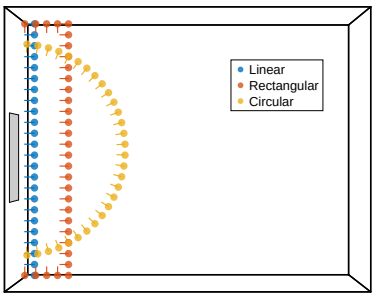

Figure 3: Evaluated loudspeaker array geometries in front of the window in the sending room.

2.3 Speaker Array Geometries

In previous research utilizing the Living Room Lab, we used a linear loudspeaker array of 24 studio loudspeakers [14]. However, during an informal validation presented in [15], we found that such a linear speaker arrangement is not ideal for synthesizing vehicle passages parallel to the loudspeaker array, especially when large incidence angles are of interest. The larger the angle between the virtual sound source and the normal vector of each loudspeaker membrane, the smaller the pressure gradient that is synthesized by each loudspeaker. If the linear array were of infinite length, or at least of similar length as the traveled distance of the vehicle, there would always be some loudspeaker positions synthesizing a large pressure gradient, resulting in an overall accurate sound field reproduction. In the Living Room Lab, the length of the linear loudspeaker array is limited to 3.7 m, which means that long vehicle passages are distorted in their time structure as visualized in Figure 2. This shortcoming of finite linear loudspeaker arrays is also known as "aperture effect" and even though applying tapering windows may reduce some of the artifacts caused by spatial truncation, conventional wave field synthesis does not offer any solution to avoid this overall level reduction for large incidence angles [10].

A straightforward solution to accurately synthesize long vehicle passages might be to use a different loudspeaker geometry, such as the rectangular and circular geometries shown in Figure 3. These geometries ensure that some loudspeakers are always oriented toward the virtual sound source and, hence, exhibit a large pressure gradient. Even though one might assume that, under ideal free-field conditions, a circular array, as shown in Figure 3, is superior to a linear or a rectangular array, it is not easy to predict how significant these differences actually would be in the lab setup, considering the propagation through the window and reflections in source and receiver room, and whether these differences are audible. Therefore, the main research question of this paper is to evaluate how these different array geometries affect the final vehicle pass-by auralization both numerically and perceptually. To avoid potential differences in spatial aliasing, the distance between all loudspeakers was set to 15.5 cm for all array geometries, resulting in a spatial aliasing frequency of approximately 1100 Hz. Maintaining the same distance resulted in the linear array consisting of 24, the circular array of 30, and the rectangular array of 32 loudspeakers.

2.4 Numerical Model

To evaluate which speaker geometry is most suitable for the auralization of vehicle pass-bys in the Living Room Lab, a numerical model of the entire transmission path from the loudspeakers in the source room through the window to a listening position in the receiving room was set up. As a "ground-truth" reference, a model with a free-field on the outdoor side and a continuous source movement instead of the wave field synthesis was created. This allows for investigating how much the limited size and resolution of the loudspeaker array, in combination with unwanted reflections in the source room, affect the result in the receiving room compared to an ideal free-field case. Figure 4 shows an example of the capabilities of this model, illustrating the instantaneous sound field in source and receiver rooms as well the velocity on the window for a circular loudspeaker array synthesizing a 600 Hz sine wave impinging from above. Even though Figure 4 is simplified to a 2D representation, the numerical model is defined and solved in 3D, as described in the following.

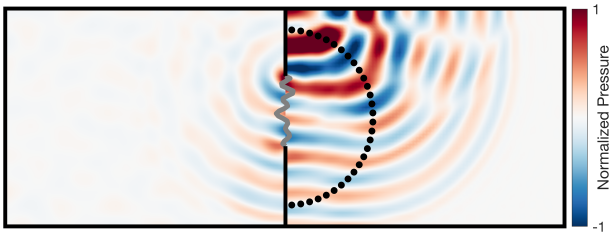

Figure 4: Simulated instantaneous pressure distribution in source and receiver room for 600 Hz sine wave impinging from the top, synthesized by circular WFS array. The shape of the grey line visualizes the window surface velocity.

Assuming a point source at position s in the sending room, the resulting pressure at an arbitrary point m on the window, $p_{s,m}$, excites the window to vibrate with a surface normal velocity, u_m, which then leads to sound radiation in the receiving room. The airborne radiation from any point m on the window to another point n on the window can be described by a Green's function, $G_{m,n}$, obtained through a modal superposition approach for a rectangular room including a frequency-dependent loss factor [16, 4.4.2]. The radiation from a vibrating window point m to any point in the receiving room r, $G_{m,r}$, and the radiation from the source position to any point on the window, $G_{s,m}$, can be calculated similarly. This approach is computationally expensive but can be optimized since, for all Green's functions of interest, either the source or the receiver is placed on the room boundary, i.e., the window. This allows for assuming plane wave propagation in one room dimension, reducing computational complexity. Finally, exciting the window at one point m will lead to structure-born sound transmission to another window point n described by the transfer mobility $Y_{m,n}$, which can be approximated by the analytical solution for a simply supported plate based on the Euler-Bernoulli theory. Within this model, three equations can be set up:

Firstly, the sending room pressure on a point n on the window, $p_{1,n}$, equals the source pressure plus the sum of the airborne contribution of all vibrating points of the window on the source side, $G_{1,m,n}$.

$$p_{1,n} = p_{s,n} + \sum_m u_m \cdot G_{1,m,n} \tag{1}$$

Secondly, the receiving room pressure on a point n on the window, $p_{2,n}$, equals the sum of the airborne contribution of all vibrating points on the receiving side of the window, $G_{2,m,n}$.

$$p_{2,n} = \sum_m u_m \cdot G_{2,m,n} \tag{2}$$

Thirdly, the surface normal velocity of one vibrating point equals the sum of the difference between indoor and outdoor pressure times the corresponding transfer mobility, $Y_{n,m}$.

$$u_m = \sum_n Y_{n,m} \cdot (p_{1,n} - p_{2,n}) \tag{3}$$

These three equations result in a linear equation system that can be solved in the frequency domain for the surface normal velocity of each point of the vibrating window u_m. The pressure p_r at a receiving position, r, can then be calculated as

$$p_r = \sum_m u_m \cdot G_{m,r}. \tag{4}$$

This allows for calculating transfer functions from all source loudspeaker positions to arbitrary points in the receiving room. To generate a reference free-field scenario, the diffuse Green's functions in the source room, $G_{s,m}$ and $G_{1,m,n}$, are replaced by free-field monopole radiation.

2.5 Auralization

While the model described in Section 2.4 allows for numerically comparing vehicle passages synthesized with different speaker geometries to a continuous free-field case, such a numerical simulation alone might not be conclusive as to whether potential differences are actually audible. Therefore, the *Chalmers Auralization Toolbox* [17] was used to create binaural renderings of the different simulated passages by sampling the sound field at a receiver position using a spherical double-layer array of 81 virtual microphones. This sampled sound field data is then used as an input to a multiple-input and multiple-output (MIMO) system with the left and right ear signals as output. The transfer functions between the input and the output are computed through a least-squares fit on sampled HRTF data, in this case, measurements of a Neumann KU100 artificial head [18]. Combining the transfer functions obtained from the numerical model with this direct auralization method results in a set of binaural room impulse responses (BRIRs) that describe the propagation from each of the loudspeakers through the window to a listener's ears in the receiver room.

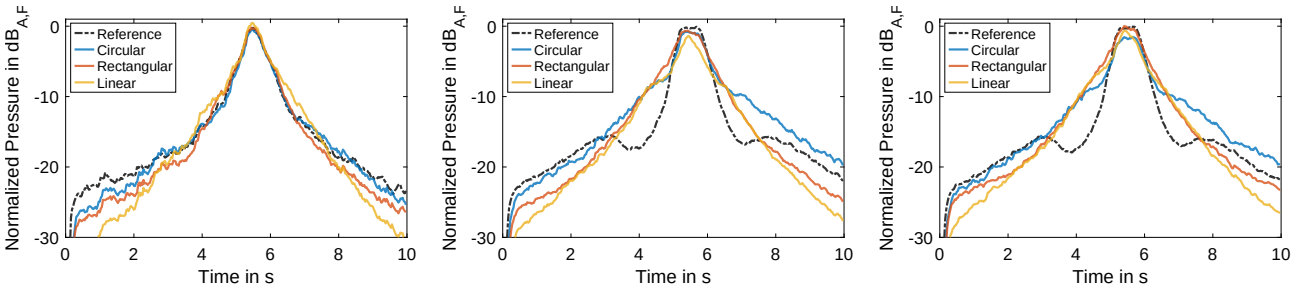

Figure 5: Normalized sound pressure level in receiving room for 25 km/h pass-by at 7.5 m distance using free-field 1 kHz pink noise (a), free-field 4 kHz pink noise (b), and 4 kHz pink noise in sending room (c).

2.6 Perceptual Validation

For a perceptual validation, 10 s long binaural stimuli simulating 25 km/h passages at 7.5 m street distance were generated using a two-tone AVAS, a multi-tone AVAS, a noise AVAS, and a combustion engine noise utilizing the binaural transfer functions obtained as described in Section 2.5. The AVAS signals were generated using an EV auralization toolbox published in [7], and the combustion engine sounds are based on recordings presented in [4]. All passages included noise from four uncorrelated tires that were treated as separate sound sources. Motivated by boundary element simulations performed in [7], a slight frequency-dependent cardioid directivity was assumed for the AVAS/combustion sound, and a measured directivity was applied for the tires. All stimuli were generated by simulating wave field synthesis via a linear, rectangular, and circular WFS array in the sending room and for a continuous free-field case to serve as ground truth. Additionally, a slower 10 km/h passage and a mono version of the continuous free-field reference were generated to serve as low-quality anchors in the perceptual comparison. All signals were normalized to a peak sound pressure level of 50 $\mathrm{dB_{A,F}}$ and are openly accessible at `doi.org/10.5281/zenodo.15102179`.

In the experiment, participants were asked to rate the similarity of the four different reproduction methods (linear array WFS, rectangular array WFS, circular array WFS, free-field continuous) as well as those two low-quality anchors (10 km/h free-field continuous and mono version of 25 km/h free-field continuous) to the free-field continuous reference. This comparison was done separately for the four different source signals (combustion, two-tone AVAS, multi-tone AVAS, noise AVAS), and the order of stimuli within these comparisons was randomized for each participant. The stimuli were presented via calibrated headphones using a HeadAcoustics SQala jury testing system and assuming a static head position.

Participants rated the similarity to the reference on an 11-point Likert scale ranging from “not at all similar” to “extremely similar”. The experiment was performed by 15 participants (8 Female, 7 Male) between 21 and 64 years old, with a median age of 27 years and self-reported normal hearing.

3. RESULTS

3.1 Numerical Results

3.1.1 Low-pass Noise Assuming Outdoor Free-Field

The simplest scenario to investigate is to omit the effects of the sending room, i.e., assume free-field conditions on the outdoor side of the window and generate a vehicle passage using a simple low-pass filtered pink noise as the source signal for a 25 km/h pass-by at 7.5 m street distance. Figure 5a shows the numerical results for normalized time-weighted sound pressure level at a position in the receiving room, comparing the three evaluated array geometries to a continuous reference. This outcome is very similar to the simulations generated in complete free-field without any room or window modeling shown in Figure 2, and confirms that the expected time structure distortions due to a finite array size are also visible when the sound propagates through a window in a receiving room. As hypothesized in Section 2.3, the linear loudspeaker array shows the strongest attenuation for large incidence angles, i.e., at the beginning and the end of the passage, and the circular array is most similar to the reference.

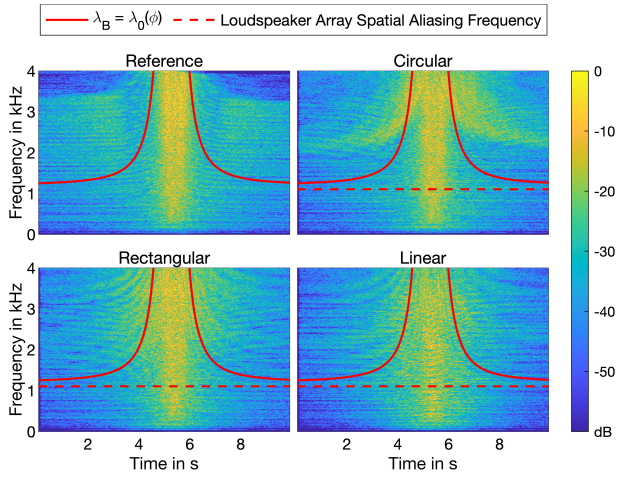

Figure 6: Spectrograms of normalized sound pressure in receiver room for 25 km/h pass-by at 7.5 m distance using 4 kHz pink noise as source signal and assuming free-field conditions on the outdoor side.

3.1.2 Broadband Noise Assuming Outdoor Free-Field

Simulating a 4 kHz pink noise passage while assuming free-field conditions on the outdoor side reveals two different phenomena that affect the time structure of the sound pressure level in the receiving room. As shown in Figure 5b, the sound pressure level of the continuous reference signal shows a dip around 4 s and 7 s that does not occur in the reference results for a 1 kHz band-limited noise passage shown in Figure 5a. This dip is caused by the fact that the coupling between an incoming airborne sound pressure wave and the bending waves on the vibrating window depends on the angle of incidence [16, Sec. 6.5] and is also visible when analytically calculating the sound reduction index for an infinitely large plate [16, Eq. 6.98]. At one specific combination of frequency and angle of incidence, ϕ, the wavelength of the airborne sound projected to the window, λ_0, exactly fits the bending wavelength on the window, λ_B, which means that the coupling between airborne and structure-borne sound is ideal and more sound is transmitted through the window. The frequency at which this coincidence effect occurs depends on the vehicle position during a passage and is illustrated by the solid red lines in Figure 6. Together with the angle-dependent pressure gradient of the incoming wavefront and the circumstance that the source distance changes throughout a pass-by, the combination of these effects results in the observed dip in the sound pressure level.

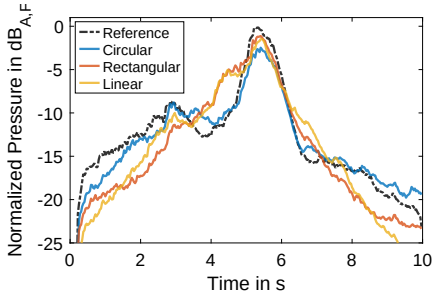

Figure 7: Normalized sound pressure level for combustion vehicle pass-by, including tire noise, directivities, air attenuation, and sending room reflections.

A second consequence of increasing the source signal frequency is the occurrence of spatial aliasing due to the limited number of loudspeakers. This is visible when comparing the reference spectrogram in Figure 6 to the WFS results and might also contribute to the deviations in the overall sound pressure level shown in Figure 5b. Additionally, this spatial aliasing causes the pressure field in front of the window to not purely consist of waves impinging from the same angle of incidence, which might explain why the WFS renderings do not exhibit as strong of a coincidence effect as the continuous reference.

3.1.3 Broadband Noise Including Sending Room

Including the sending room contributions in the model slightly increases the overall sound pressure level at the beginning and end of the vehicle passage for all three array geometries, as shown in Figure 5c. This is to be expected as the reflections in the sending room are strongest for the loudspeakers close to the room corners, which are mostly used for large incidence angles (see, e.g., the sound field shown in Figure 4). However, just considering the time structure of the overall sound pressure level at a single position in the receiver room, the influence of the sending room seems to be relatively small when comparing Figure 5b and Figure 5c.

3.1.4 Vehicle Passage Including Sending Room

Figure 7 shows the simulated normalized sound pressure level at a receiving room position for a complete combustion engine vehicle pass-by, including four uncorrelated tire noise sources, air attenuation, and motor and tire directivities. Even though this scenario is the most relevant for our intended application, including all of these factors increases the complexity of the indoor noise time structure, making it challenging to interpret deviations between the reference and the WFS result. While it is evident

that none of the WFS renderings exactly match the reference results, the circular loudspeaker array produces the most accurate overall representation for this specific simulation, considering only the course of the overall sound pressure level. However, these results alone do not indicate whether deviations between the different WFS setups are audible and could affect how subjects perceive the auralized passages in a listening experiment. While these simulations provide a better understanding of the underlying mechanisms and limitations of the Living Room Lab, only the perceptual results presented in the following allow for judging the perceived quality of the auralizations.

3.2 Perceptual Results

Figure 8 shows the results of the listening experiment, where participants judged how similar they perceived auralizations via the three different WFS array geometries, a hidden reference, and two low-quality anchors compared to a free-field continuous reference passage. The triangular markers represent the arithmetic mean for different source signal types, and the circular markers with error bars represent the arithmetic mean and 95% confidence intervals for the combination of all evaluated source types.

After averaging the responses of the four different sound types for each participant, a repeated measures ANOVA confirmed a significant main effect of the auralization type on the perceived similarity to the continuous free-field reference ($F(5, 70) = 18.14, p < .001, \eta_p^2 = 0.56$). Bonferroni corrected post-hoc tests showed significant differences between the reference sound and all other stimuli, as well as between the low-speed anchor and the rectangular and circular WFS rendering methods.

From these results, it is evident that the participants successfully identified the hidden reference, i.e., they rated the similarity between the reference and the stimulus that was exactly the same as the reference as the highest. Additionally, the low-speed and mono anchors were rated as significantly lower in similarity, confirming that participants generally could perceive differences between the presented stimuli. However, the results for the three different WFS renderings are less conclusive as they are rated significantly lower than the hidden reference but higher than the low-quality anchors while not showing any statistically significant differences between the different WFS geometries. Even though not significant, the mean similarity for the linear array is lower than for the rectangular and circular arrays, which is consistent with the numerical results presented in Section 3.1.

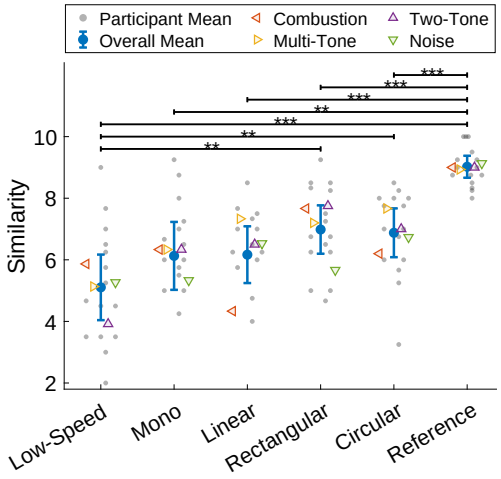

Figure 8: Similarity ratings averaged over stimuli types for each participant, overall mean with 95% confidence intervals, and mean values for each stimulus type. Horizontal bars indicate significant paired comparisons of overall means (** $p < .01$, *** $p < .001$).

4. DISCUSSION

Based on the numerical results and especially when considering low-passed noise in free-field conditions, the circular loudspeaker array auralizations were most similar to the simulated continuous reference passage. However, including the sending room contributions, separate sound sources for tires and propulsion, and directivities in the auralization makes it challenging to determine which WFS geometry is favorable and how severe the differences are. The magnitude of the deviations between reference and WFS renderings also depends on the overall duration and speed of the pass-by. For the extreme case shown in Figure 2, the vehicle reaches a position of 70 m at 7.5 m street distance, corresponding to a large incidence angle that a linear WFS array can not synthesize. For research regarding the perception of electric vehicle noise, however, slower passages are of interest, which, as seen in Figure 5a, do not exhibit that strong of a time structure distortion. Additionally, all presented simulations only consider a single position in the receiver room, which, even though realistic for upcoming experiments in the lab, means that the results may differ for other positions. Nevertheless, while room modes and window radiation might affect the spectral balance depending on the exact evaluated position in the receiver room, we do not expect the observed trends for the overall sound pressure level to deviate much.

The perceptual results show that, although participants could identify differences between the presented auralizations and the reference, there is no significant difference between the similarity ratings of the different array geometries. However, these findings only apply to pass-by auralizations at realistic indoor sound levels. As such, the presented signals were relatively quiet. Increasing the level and using a simple noise signal, such as the pink noise shown in Figure 5c, or only presenting short excerpts instead of complete vehicle passages might have increased the audible differences. Apart from a few very experienced listeners, most participants reported after the experiment that they barely perceived any differences and found it challenging to judge which signals sounded more or less similar to the reference. This ambiguity underlines that such listening experiments depend highly on the recruited participant group. For this study, the subject group consisted of four experienced acoustics researchers and 11 acoustics Master's students with less experience in critical listening. While this group is representative for the participants we plan to use in upcoming EV experiments, the results of the perceptual evaluation would most likely differ when only using expert listeners or recruiting a group of entirely inexperienced subjects.

5. CONCLUSION

This paper compared different WFS loudspeaker geometries for vehicle pass-by auralizations through a window in a transmission suite. While numerical simulations indicated that a circular loudspeaker array setup results in auralizations more similar to a continuous free-field reference than a linear or rectangular speaker array geometry, a perceptual evaluation did not reveal significant differences between those setups. We therefore conclude that, if possible, a circular setup should be used for vehicle pass-by auralizations. However, based on the perceptual judgments of a mixed group of expert and non-expert listeners, we do not expect significantly less plausible results from the linear or rectangular setups in this specific application.

6. ACKNOWLEDGMENTS

This research was funded by FORMAS, a Swedish research council for sustainable development (FR-2020-01931). The HEAD-Genuit Foundation provided the hardware used for the listening experiment (P-22101-W).

7. REFERENCES

[1] M.-A. Pallas, M. Bérengier, R. Chatagnon, M. Czuka, M. Conter, and M. Muirhead, "Towards a model for electric vehicle noise emission in the European prediction method CNOSSOS-EU," *Applied Acoustics*, vol. 113, pp. 89–101, 2016.

[2] UNECE, "Regulation No 138 — Uniform provisions concerning the approval of Quiet Road Transport Vehicles with regard to their reduced audibility," tech. rep., 2017.

[3] R. W. Emerson, D. S. Kim, K. Naghshineh, J. Pliskow, and K. Myers, "Detection of Quiet Vehicles by Blind Pedestrians," *Journal of Transportation Engineering*, vol. 139, no. 1, pp. 50–56, 2013.

[4] L. Müller, J. Forssén, and W. Kropp, "Auditory localization of multiple stationary electric vehicles," *The Journal of the Acoustical Society of America*, vol. 157, no. 3, pp. 2029–2041, 2025.

[5] NHTSA, "Minimum Sound Requirements for Hybrid And Electric Vehicles - Final Environmental Assessment," tech. rep., National Highway Traffic Safety Administration.

[6] M. E. Altinsoy, "The Evaluation of Conventional, Electric and Hybrid Electric Passenger Car Pass-By Noise Annoyance Using Psychoacoustical Properties," *Applied Sciences*, vol. 12, no. 10, 2022.

[7] L. Müller and W. Kropp, "Auralization of electric vehicles for the perceptual evaluation of acoustic vehicle alerting systems," *Acta Acustica*, vol. 8, p. 27, 2024.

[8] L. Müller and W. Kropp, "On the influence of AVAS directivity on electric vehicle speed perception," in *INTER-NOISE and NOISE-CON Congress and Conference Proceedings*, vol. 270, 2024.

[9] E. Verheijen, *Sound Reproduction by Wave Field Synthesis*. PhD thesis, 1998. Delft University of Technology.

[10] J. Ahrens, *Analytic Methods of Sound Field Synthesis*. Springer Berlin Heidelberg, 2012.

[11] S. Spors and J. Ahrens, "Analysis and Improvement of Pre-Equalization in 2.5-Dimensional Wave Field Synthesis," in *128th Convention of the AES*, 2010.

[12] "ISO 9613-1:1993 Acoustics — Attenuation of sound during propagation outdoors — Part 1: Calculation of the absorption of sound by the atmosphere," tech. rep., 1993.

[13] F. Rietdijk, K. Heutschi, and J. Forssén, "Modelling sound propagation in the presence of atmospheric turbulence for the auralization of aircraft noise," *The Journal of the Acoustical Society of America*, vol. 136, no. 4, pp. 2286–2286, 2014.

[14] L. Müller, J. Forssén, and W. Kropp, "Traffic Noise at Moderate Levels Affects Cognitive Performance: Do Distance-Induced Temporal Changes Matter?," *International Journal of Environmental Research and Public Health*, vol. 20, no. 5, p. 3798, 2023.

[15] L. Müller, W. Kropp, and J. Forssén, "Measurement, Simulation and Auralization of Indoor Road Traffic Noise," in *DAGA 2022*, 2022.

[16] T. E. Vigran, *Building Acoustics*. Taylor & Francis, 2008.

[17] J. Ahrens, "Perceptually Transparent Binaural Auralization of Simulated Sound Fields," *arXiv*, 2024.

[18] B. Bernschütz, "A Spherical Far Field HRIR/HRTF Compilation of the Neumann KU 100," in *AIA-DAGA Fortschritte der Akustik*, (Merano), 2013.